Structural Eng./Earthquake Eng. Vol. 9, No. 3, 203s—211s, October 1992
Japan Society of Civil Engineers (Proc. of JSCE No. 455/I—21)

ANALYSIS ON GEOMETRICAL NONLINEAR BEHAVIOR OF RECTANGULAR PLATES

Chihiro MORITA*, Hiroshi MATSUDA**
and Takeshi SAKIYAMA***

In this paper, a dicsrete method for analyzing the geometrical nonlinear problems of rectangular plates is proposed. The solutions of partial differential equations of rectangular plates are obtained in discrete forms by applying the numerical integration, and they give the transverse shear forces, twisting moment, bending moments, rotations, deflection, in-plane displacements and membrane forces at all discrete points. The nonlinear problems are solved by the iteration and the load incremental procedure.
As the applications of the present method, geometrical nonlinear bending and post-buckling problems of rectangular plates with some of boundary conditions are calculated.
Key words *: geometrical nonlinear, post-buckling, a discrete method*

1. INTRODUCTION

The fundamental equations for large deflection of the rectangular plates have been derived by von Kármán [1], and the extension to the plate with small initial curvature has been achieved by Marguerre [2].

Using these equations, the geometrical nonlinear problems of the rectangular plates have been analyzed by many researchers. The approximate solutions of the rectangular plate subjected to lateral loads have been obtained by the finite element method[3),4)], the energy method[5)], etc.[6),7)]. The post-buckling behavior of the rectangular plate under edge compression has been investigated by using the numerical methods such as the finite element method[8)], the finite strip method[9)], etc. [10),11)].

However, it has been hardly carried out to studies the geometrical nonlinear problems of the plates having various boundary and loading conditions.

In this paper, a discrete method is developed to study the geometrical nonlinear analysis of the rectangular plate. The discrete solutions of partial differential equations governing the geometrical nonlinear behavior of the rectangular plate are obtained in discrete forms. By transforming the differential equations into integral equations and applying numerical integrations, the discrete solutions can be obtained. Thus, they give the transverse shear forces, twisting moment, bending moments, rotations, deflection, in-plane displacements and membrane forces at all discrete points of the plate.

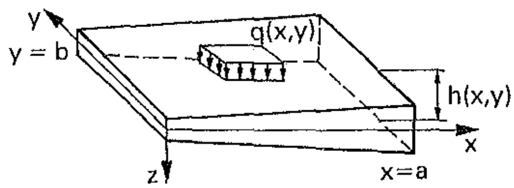

Fig.1 Rectangular plate and coordinate system.

As the applications of the proposed method, numerical solutions for square plates with three types of boundary conditions : four clamped edges, four simply supported edges, and two opposite edges simply supported and the other two edges clamped, are presented.

2. FUNDAMENTAL DIFFERENTIAL EQUATIONS

A rectangular Mindlin plate is referred to an *x-y-z* system of rectangular coordinates with the position of the origin 0 of the *x-y-z* system at the corner of the middle plane of the plate, as shown in **Fig.1**. The fundamental differential equations governing the geometrical nonlinear bending of the rectangular plates which are subjected to the distributed lateral load $q(x,y)$ and the membrane forces N_{xy}, N_y and N_x are given as Eqs.(1.a)~(1.h). These equations are based

* Member of JSCE, M.Eng., Research Associate, Dept. of Structural Eng., Nagasaki Univ. (1-14 Bunkyou-machi, Nagasaki 852)
** Member of JSCE, Dr.Eng., Associate Professor, Dept. of Structural Eng., Nagasaki Univ.
*** Member of JSCE, Dr.Eng., Professor, Dept. of Structural Eng., Nagasaki Univ.

on Mindlin's theory which includes the effects of shear deformations. Since an incremental procedure is used in nonlinear calculation, the fundamental differential equations are presented in following incremental forms.

$$\frac{\partial \Delta Q_x}{\partial x}+\frac{\partial \Delta Q_y}{\partial y}-\frac{N_x-\nu N_y}{(1-\nu^2)D}\Delta M_x-\frac{N_y-\nu N_x}{(1-\nu^2)D}\Delta M_y-\frac{2N_{xy}}{(1-\nu)D}\Delta M_{xy}+\Delta q+\Delta N_c=0 \quad \cdots (1.a)$$

$$\frac{\partial \Delta M_x}{\partial x}+\frac{\partial \Delta M_{xy}}{\partial y}-\Delta Q_x=0 \quad \cdots\cdots\cdots\cdots (1.b)$$

$$\frac{\partial \Delta M_y}{\partial y}+\frac{\partial \Delta M_{xy}}{\partial x}-\Delta Q_y=0 \quad \cdots\cdots\cdots\cdots (1.c)$$

$$\frac{\partial \Delta \theta_x}{\partial x}+\nu\frac{\partial \Delta \theta_y}{\partial y}=\frac{\Delta M_x}{D} \quad \cdots\cdots\cdots\cdots\cdots (1.d)$$

$$\frac{\partial \Delta \theta_y}{\partial y}+\nu\frac{\partial \Delta \theta_x}{\partial x}=\frac{\Delta M_y}{D} \quad \cdots\cdots\cdots\cdots\cdots (1.e)$$

$$\frac{\partial \Delta \theta_x}{\partial y}+\frac{\partial \Delta \theta_y}{\partial x}=\frac{2\Delta M_{xy}}{(1-\nu)D} \quad \cdots\cdots\cdots\cdots (1.f)$$

$$\frac{\partial \Delta w}{\partial x}+\Delta\theta_x=\frac{\Delta Q_x}{\kappa Gh} \quad \cdots\cdots\cdots\cdots\cdots\cdots (1.g)$$

$$\frac{\partial \Delta w}{\partial y}+\Delta\theta_y=\frac{\Delta Q_y}{\kappa Gh} \quad \cdots\cdots\cdots\cdots\cdots\cdots (1.h)$$

The relation between in-plane displacements u, ν and membrane forces N_{xy}, N_y and N_x are expressed as follows :

$$\frac{\partial \Delta N_x}{\partial x}+\frac{\partial \Delta N_{xy}}{\partial y}=0 \quad \cdots\cdots\cdots\cdots\cdots\cdots (1.i)$$

$$\frac{\partial \Delta N_y}{\partial y}+\frac{\partial \Delta N_{xy}}{\partial x}=0 \quad \cdots\cdots\cdots\cdots\cdots\cdots (1.j)$$

$$\frac{\partial \Delta u}{\partial x}+\nu\frac{\partial \Delta v}{\partial y}+\Delta W_{xc}=\frac{\Delta N_x}{F} \quad \cdots\cdots\cdots (1.k)$$

$$\frac{\partial \Delta v}{\partial y}+\nu\frac{\partial \Delta u}{\partial x}+\Delta W_{yc}=\frac{\Delta N_y}{F} \quad \cdots\cdots\cdots (1.l)$$

$$\frac{\partial \Delta u}{\partial y}+\frac{\partial \Delta v}{\partial x}+\Delta W_{xyc}=\frac{2\Delta N_{xy}}{(1-\nu)F} \quad \cdots\cdots (1.m)$$

where Q_y,Q_x : transverse shear forces, M_{xy} : twisting moment, M_y,M_x : bending moments, θ_y,θ_x : rotations, w : deflection, v,u : in-plane displacements, N_{xy},N_y,N_x : membrane forces, $D=Eh^3/[12(1-\nu^2)]$: flexural rigidity of the plate, E : modulus of elasticity, $G=E/[2(1+\nu)]$: shear modulus of elasticity, h : thickness of the plate, ν : Poisson's ratio, $\kappa=5/6$: shear coefficient, $F=Eh/(1-\nu^2)$, $\Delta Q_y,\Delta Q_x$ = increments of shear forces Q_y,Q_x ; $\Delta M_{xy},\Delta M_y,\Delta M_x$ = increments of moments M_{xy},M_y,M_x ; $\Delta\theta_y,\Delta\theta_x$ = increments of rotations θ_y,θ_x ; Δw = increment of deflection w ; $\Delta v,\Delta u$ = increments of in-plane displacements v,u ; $\Delta N_{xy},\Delta N_y,\Delta N_x$ = increments of membrane forces N_{xy},N_y,N_x ; Δq = increment of load q, $\Delta N_c,\Delta W_{xyc},\Delta W_{yc},\Delta W_{xc}$ = unbalanced force and nonlinear terms (APPENDIX I).

By using the following non-dimensional expression,

$$X_1=a^2Q_y/[D_0(1-\nu^2)],\ X_2=a^2Q_x/[D_0(1-\nu^2)],$$
$$X_3=aM_{xy}/[D_0(1-\nu^2)],\ X_4=aM_y/[D_0(1-\nu^2)],$$
$$X_5=aM_x/[D_0(1-\nu^2)],\ X_6=\theta_y,\ X_7=\theta_x,$$
$$X_8=w/a,\ \eta=x/a,\ \zeta=y/b$$

the differential Eqs.(1.a)~(1.h) are rewritten as follows:

$$\sum_{s=1}^{8}\left[F_{1ts}\frac{\partial \Delta X_s}{\partial \zeta}+F_{2ts}\frac{\partial \Delta X_s}{\partial \eta}+F_{3ts}\Delta X_s\right]+f_{1t}=0 \quad \cdots\cdots (2.A)$$
$$(t=1,2,\cdots,8)$$

Similarly, by using the following non-dimensional expression,

$$X_9=v/a,\ X_{10}=u/a,\ X_{11}=a^2N_{xy}/[D_0(1-\nu^2)],$$
$$X_{12}=a^2N_y/[D_0(1-\nu^2)],\ X_{13}=a^2N_x/[D_0(1-\nu^2)]$$

the differential Eqs.(1.i)~(1.m) are rewritten as follows:

$$\sum_{s=9}^{13}\left[F_{4ts}\frac{\partial \Delta X_s}{\partial \zeta}+F_{5ts}\frac{\partial \Delta X_s}{\partial \eta}+F_{6ts}\Delta X_s\right]+f_{2t}=0 \quad \cdots\cdots (2.B)$$
$$(t=9,10,\cdots,13)$$

where a and b are length and width of the plate, $\mu=b/a$, h_0 is the standard plate thickness, D_0 is the standard flexural rigidity of the plate, $D_0=Eh_0^3/[12(1-\nu^2)]$, $\bar{D}=(h_0/h)^3$, $I=\mu(1-\nu^2)(h_0/h)^3$, $J=2\mu(1+\nu)(h_0/h)^3$, $K=Eh_0^3/(12\kappa Ga^2h)$, $L_1=\mu(1-\nu^2)h_0^3/(12a^2h)$, $L_2=\mu(1+\nu)h_0^3/(6a^2h)$, $\bar{q}=\mu qa^3/[D_0(1-\nu^2)]$, $\bar{N}_c=\mu N_c a^3/[D_0(1-\nu^2)]$, F_{kts}, f_{kt} are defined in APPENDIX II

3. DISCRETE SOLUTIONS OF DIFFERENTIAL EQUATIONS

A rectangular plate can be divided in the η-direction into m equal-length parts and in the ζ-direction into n equal-length parts as shown in **Fig.2**, and the plate considerd as a group of discrete points which are the intersections of the vertical and horizontal dividing lines.

The rectangular area, $0\le\eta\le\eta_i$ and $0\le\zeta\le\zeta_j$, corresponding to an arbitrary intersection (i,j) shown in **Fig.2**, is expressed as the area $[i,j]$ in this paper, and the intersection (i,j) denoted by ◉ is called the main point of the area $[i,j]$, and the intersections denoted by ○ as the inner dependent points, the intersections denoted by ● as the boundary de-

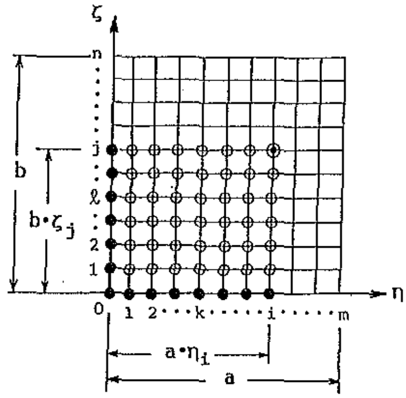

Fig. 2 Discrete points on rectangular plate.

pendent points.

By integrating Eqs.(2.A) and (2.B) over the area $[i,j]$, the following integral equations are obtained.

$$\sum_{s=1}^{8}\left\{F_{1ts}\int_0^{\eta_i}[\Delta X_s(\eta,\zeta_j)-\Delta X_s(\eta,0)]d\eta\right.$$
$$+F_{2ts}\int_0^{\zeta_j}[\Delta X_s(\eta_i,\zeta)-\Delta X_s(0,\zeta)]d\zeta$$
$$\left.+F_{3ts}\int_0^{\eta_i}\int_0^{\zeta_j}\Delta X_s(\eta,\zeta)d\eta d\zeta\right\}$$
$$+\int_0^{\eta_i}\int_0^{\zeta_j}f_{1t}(\eta,\zeta)d\eta d\zeta=0 \quad\cdots\cdots\cdots (3.A)$$

$$\sum_{s=9}^{13}\left\{F_{4ts}\int_0^{\eta_i}[\Delta X_s(\eta,\zeta_j)-\Delta X_s(\eta,0)]d\eta\right.$$
$$+F_{5ts}\int_0^{\zeta_j}[\Delta X_s(\eta_i,\zeta)-\Delta X_s(0,\zeta)]d\zeta$$
$$\left.+F_{6ts}\int_0^{\eta_i}\int_0^{\zeta_j}\Delta X_s(\eta,\zeta)d\eta d\zeta\right\}$$
$$+\int_0^{\eta_i}\int_0^{\zeta_j}f_{2t}(\eta,\zeta)d\eta d\zeta=0 \quad\cdots\cdots\cdots (3.B)$$

By applying the numerical integration to Eqs.(3.A) and (3.B), the simultaneous equation of unknown quantities X_{sij} (s=1~8,9~13) which are the dimensionless shear forces, twisting moment, bending moments, rotations, deflection, in-plane displacements and membrane forces at the main point (i,j) of the area $[i,j]$ are obtained as follows:

$$\sum_{s=1}^{8}\left\{F_{1ts}\sum_{k=0}^{i}\beta_{ik}[\Delta X_{skj}-\Delta X_{sk0}]\right.$$
$$+F_{2ts}\sum_{l=0}^{j}\beta_{jl}[\Delta X_{sil}-\Delta X_{s0l}]$$
$$\left.+F_{3ts}\sum_{k=0}^{i}\sum_{l=0}^{j}\beta_{ik}\beta_{jl}\Delta X_{skl}\right\}$$
$$+\sum_{k=0}^{i}\sum_{l=0}^{j}\beta_{ik}\beta_{jl}f_{1tkl}=0 \quad\cdots\cdots\cdots\cdots\cdots (4.A)$$

$$\sum_{s=9}^{13}\left\{F_{4ts}\sum_{k=0}^{i}\beta_{ik}[\Delta X_{skj}-\Delta X_{sk0}]\right.$$
$$+F_{5ts}\sum_{l=0}^{j}\beta_{jl}[\Delta X_{sil}-\Delta X_{s0l}]$$
$$\left.+F_{6ts}\sum_{k=0}^{i}\sum_{l=0}^{j}\beta_{ik}\beta_{jl}\Delta X_{skl}\right\}$$
$$+\sum_{k=0}^{i}\sum_{l=0}^{j}\beta_{ik}\beta_{jl}f_{2tkl}=0 \quad\cdots\cdots\cdots\cdots\cdots (4.B)$$

The solutions X_{pij} of the simultaneous Eqs. (4.A) and (4.B) are expressed as follows:

$$\Delta X_{pij}=\sum_{t=1}^{8}\left\{\sum_{k=0}^{i}A_{pt}\beta_{ik}[\Delta X_{tk0}-\Delta X_{tkj}(1-\delta_{ki})]\right.$$
$$+\sum_{l=0}^{j}B_{pt}\beta_{jl}[\Delta X_{t0l}-\Delta X_{til}(1-\delta_{lj})]$$
$$\left.+\sum_{k=0}^{i}\sum_{l=0}^{j}C_{ptkl}\beta_{ik}\beta_{jl}\Delta X_{tkl}(1-\delta_{ki}\delta_{lj})\right\}$$
$$-A_{p1}\sum_{k=0}^{i}\sum_{l=0}^{j}\beta_{ik}\beta_{jl}(\Delta\bar{q}_{kl}+\Delta\bar{N}_{ckl})\cdots (5.A)$$
$$(p=1,2,\cdots,8)$$

$$\Delta X_{pij}=\sum_{t=9}^{13}\left\{\sum_{k=0}^{i}A_{pt}\beta_{ik}[\Delta X_{tk0}-\Delta X_{tkj}(1-\delta_{ki})]\right.$$
$$+\sum_{l=0}^{j}B_{pt}\beta_{jl}[\Delta X_{t0l}-\Delta X_{til}(1-\delta_{lj})]$$
$$\left.+\sum_{k=0}^{i}\sum_{l=0}^{j}C_{ptkl}\beta_{ik}\beta_{jl}\Delta X_{tkl}(1-\delta_{ki}\delta_{lj})\right\}$$
$$-\sum_{k=0}^{i}\sum_{l=0}^{j}\beta_{ik}\beta_{jl}\Delta\bar{W}_{cpkl}\quad\cdots\cdots\cdots\cdots (5.B)$$
$$(p=9,10,\cdots,13)$$

where δ is Kronecker's delta, $i=1,2,\cdots,m$, $j=1,2,\cdots,n$, $\beta_{ik}=\alpha_{ik}/m$, $\beta_{jl}=\alpha_{jl}/n$, A_{pt},B_{pt},C_{ptkl}: APPENDIX III

The coefficients β_{ik},β_{jl} are the weight coefficients of the numerical integration. The trapezoidal rule of approximate numerical integration is applied in this paper, therefore the values of α_{ik},α_{jl} are given as follows:

$$\alpha_{ik}=1-(\delta_{0k}+\delta_{ik})/2,\quad \alpha_{jl}=1-(\delta_{0l}+\delta_{jl})/2$$

In Eqs.(5.A) and (5.B), the quantities X_{pij} at the main point (i,j) of the area $[i,j]$ are related to the quantities X_{tk0} and X_{t0l} at the boundary dependent points of the area $[i,j]$ and the quantities X_{tkj},X_{til} and X_{tkl} at the inner dependent points of the area $[i,j]$. With the spreading of the area $[i,j]$ according to regular order as [1,1],[1,2],··,[1,n],[2,1],[2,2],

$\cdots$,[2, n],$\cdots$,[m,1],[m,2],$\cdots$,[m,n], the main point of smaller area becomes one of the inner dependent points of the following larger areas. Whenever one obtains the quantities X_{pij} at the main point (i,j) of the area [i,j] by using Eqs.(5.A) and (5.B) in above mentioned order, one can eliminate the quantities X_{tkj}, X_{til} and X_{tkl} at the inner dependent points of the following larger areas by substituting the obtained results into the corresponding terms of the right hand side of Eqs.(5.A) and (5.B). By repeating this process, the quantities X_{pij} at the main point is related to only the quantities X_{rf0} (r=1,3,4,6,7, 8) and X_{s0g} (s=2,3,5,6,7,8) or X_{uf0} (u=9,10,11, 12) and X_{v0g} (v=9,10,11,13) at the boundary dependent points. The results are as follows:

p=1~8

$$\Delta X_{pij} = \sum_{d=1}^{6}\left(\sum_{f=0}^{i} a_{pijfd}\Delta X_{rf0} + \sum_{g=0}^{j} b_{pijgd}\Delta X_{s0g}\right) + \Delta q_{pij} \quad \cdots\cdots (6.A)$$

p=9~13

$$\Delta X_{pij} = \sum_{d=1}^{4}\left(\sum_{f=0}^{i} a_{pijfd}\Delta X_{uf0} + \sum_{g=0}^{j} b_{pijgd}\Delta X_{v0g}\right) + \Delta q_{pij} \quad \cdots\cdots (6.B)$$

where $a_{pijfd}, b_{pijgd}, \Delta q_{pij}$ are defined in APPENDIX III

The coefficients $a_{pijfd}, b_{pijgd}, \Delta q_{pij}$ in Eqs.(6.A) and (6.B) can be independently calculated. Eqs.(6.A) and (6.B) can be recognized as the discrete solutions of the fundamental partial differential Eqs.(2.A) and (2.B).

4. INTEGRAL CONSTANTS AND BOUNDARY CONDITIONS

Integral constants X_{rf0} and X_{s0g}, or X_{uf0} and X_{v0g} express dimensionless quantities with respect to $Q_y, M_{xy}, M_y, \theta_y, \theta_x, w$ and $Q_x, M_{xy}, M_x, \theta_y, \theta_x, w$, or v, u, N_{xy}, N_y and v, u, N_{xy}, N_x on ζ=0 and η=0, respectively.

There are ten integral constants at each discrete point, and five of them are self-evident according to the boundary conditions along the edges ζ=0 and η=0. The remaining five integral constants can be determined by the boundary conditions along the edges ζ=1.0 and η=1.0.

(1) The boundary conditions of rectangular plate subjected to lateral loads

For the boundary conditions of rectangular plate subjected to lateral loads, the following four cases : four clamped edges (CCCC) ; four simply supported edges with pin supported (SSSS-pin) ; four simply supported edges with roller supported (SSSS-roller) ; two opposite edges simply supported and the other edges clamped (SCSC) are indicated. These integral constants and the boundary conditions are shown in **Fig.3**(1)~(4), respectively. These figures represent one quarter of the rectangular plate with two symmetrical axes. The integral constants and the boundary conditions at the corners of each plate are shown in the boxes. For the details of dealing with the integral constants and boundary conditions, see Ref.12).

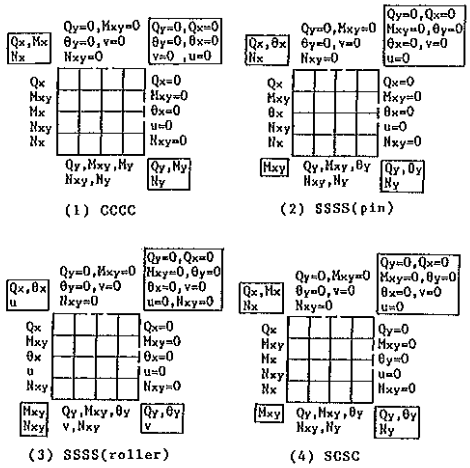

Fig.3 Integral constants and boundary conditions.

(2) The boundary conditions of rectangular plate subjected to edge compression

Concerning the loading conditions of the plate subjected to edge compression, the following cases are considered:

[Uniformly displaced edges]

along x=0, a	along y=0, b
$u = const$	$N_{xy} = 0$
$P = \int_0^b \frac{N_x}{h} dy$	$N_y = 0$
$N_{xy} = 0$	

[Uniformly loaded edges]

along x=0, a	along y=0, b
$P = const$	$N_{xy} = 0$
$N_{xy} = 0$	$N_y = 0$

As for the supporting conditions, we will treat the following three cases : a) - four simply supported edges ; b) - loaded edges clamped, the other edges simply supported ; c) - loaded edges simply supported, the other edges clamped.

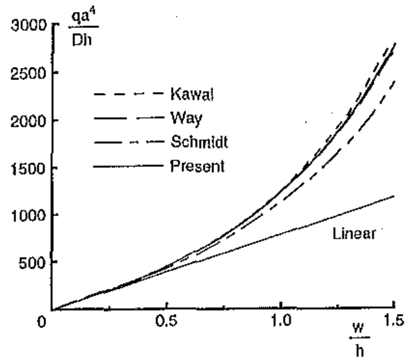

Fig.4 Load-deflection curves under uniform lateral load (CCCC).

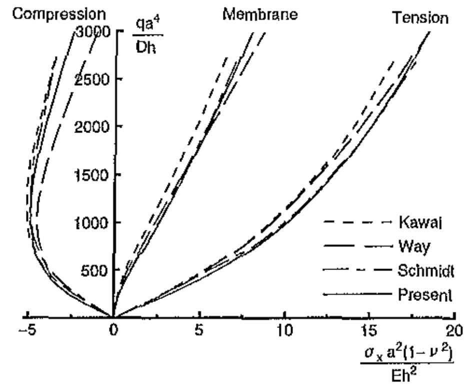

Fig.5 Load-stress curves under uniform lateral load (CCCC).

5. COMPUTATIONAL PROCEDURE

In this paper, the geometrical nonlinear problems are solved by iteration and the load incremental procedure. The outline of the computational procedure is described as follows:

1). Calculating the unbalanced force ΔN_c in Eq.(1.a), and substituting membrane forces N_x, N_y and N_{xy}, the solutions $\Delta Q_y, \Delta Q_x, \Delta M_{xy}, \Delta M_y, \Delta M_x, \Delta\theta_y, \Delta\theta_x$ and Δw for out-plane bending deformation are obtained. (Only first step, the unbalanced force ΔN_c is equal to zero.)
2). From Eqs.(1.g) and (1.h), the values $\partial w/\partial x$ and $\partial w/\partial y$ are obtained.
3). Calculating the nonlinear terms ΔW_{xc}, ΔW_{yc} and ΔW_{xyc} in Eqs.(1.k), (1.l) and (1.m), the solutions $\Delta v, \Delta u, \Delta N_{xy}, \Delta N_y$ and ΔN_x for in-plane deformation are obtained.
4). From the membrane forces $\Delta N_{xy}, \Delta N_y$ and ΔN_x, the unbalanced force ΔN_c in Eq.(1.a) is again calculated.

The iteration processes 1)~4) must continue until the unbalanced force approach to zero and the new increment of the deformations become sufficiently small.

6. NUMERICAL RESULTS

Numerical solutions for two specific problems are presented. The first problem involves the square plates subjected to lateral loads that are uniformly distributed throughout the plate or concentrated at the center of the plate. The other problem involves the square plate subjected to edge compression and with small initial curvature.

(1) Rectangular plate subjected to lateral loads

First, in order to confirm the convergence and accuracy of numerical solutions obtained by the discrete method, it is applied to the geometrical nonlinear analysis of square plates (h/a=0.01, ν=0.3) subjected to uniformly distributed lateral load. From the results of four clamped edges plate which is divided into m=n=4,6,8,10, the numerical solutions of the division m=n=8 agreed with those of m=n=10. Thus, the numerical computation for m=n=8 is carried out.

a) Plate with four clamped edges (CCCC)

Figs.4 and **5** present the computing results for a square plate with four clamped edges. **Fig.4** shows the load-deflection curves with respect to maximum deflection. **Fig.5** shows the load-stress curves at the center of the square plate with respect to upper surface (compression), lower surface (tension) and membrane stress. These figures show the comparison between the discrete solutions and the other solutions such as the finite element solutions obtained by Kawai *et al.* [3] and Schmidt [4], and the solutions from the energy method by Way [5]. It is found from these figures that the numerical solutions obtained by the discrete method agree with those obtained by finite element and the energy method.

b) Simply supported plate (SSSS)

Figs.6, 7 and 8 present the computing results for a square plate with four simply supported edges. **Fig.6** shows the load-deflection curves with respect to the maximum deflection when non-dimensional incremental load intensity is $\Delta qa^4/Dh = 100$. **Figs.** 7 and 8 shows the load-stress curves at the center of the square plate, and the former is the results of the plate with pin supported

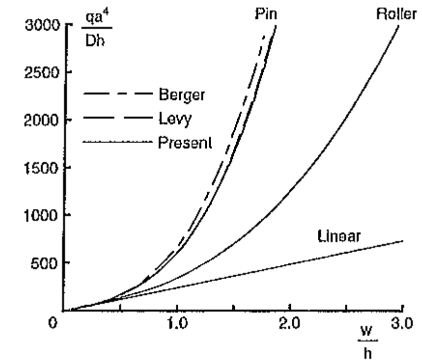

Fig.6 Load-deflection curves under uniform lateral load (SSSS).

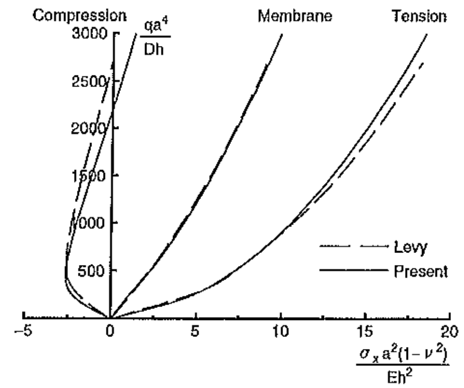

Fig.7 Load-stress curves under uniform lateral load (pin).

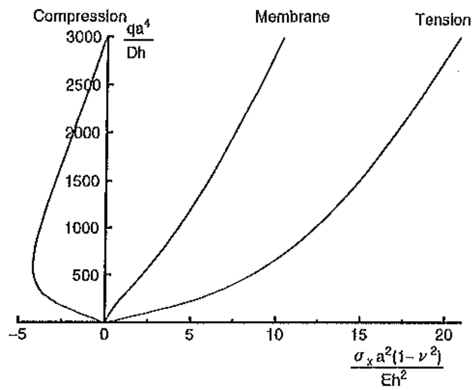

Fig.8 Load-stress curves under uniform lateral load (roller).

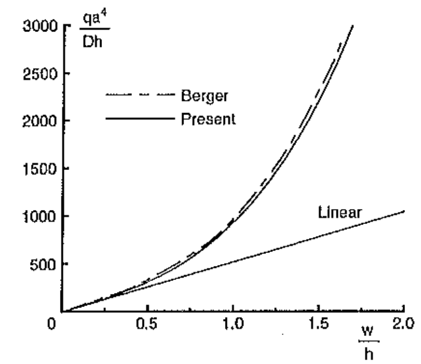

Fig.9 Load-deflection curves under uniform lateral load (SCSC).

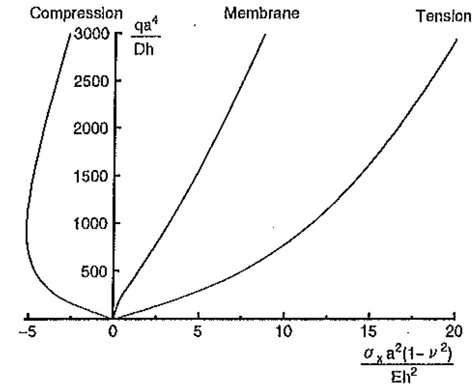

Fig.10 Load-stress curves under uniform lateral load (SCSC).

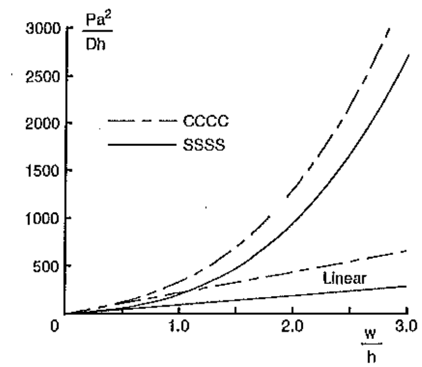

Fig.11 Load-deflection curves under a concentrated load.

edges and the latter is the results of the plate with roller supported edges. In **Figs.6** and **7**, the numerical solutions obtained from the discrete method are compared with those of the solutions by Berger[6)] and Levy[7)]. It is seen that the load-deflection curve obtained by the discrete method agree with Levy's solution better than Berger's.

c) Plate with two edges clamped (SCSC)

The results similar to those described above, for a square plate with two opposite edges simply supported and the other two edges clamped are described in **Figs.9** and **10**. **Fig.9** shows the load-deflection curves with respect to the maximum deflection when non-dimensional incremental load intensity is $\Delta qa^4/Dh = 100$. **Fig.10** shows the load-stress curves at the center of a square plate. In **Fig.9**, the numerical solutions obtained from the discrete method are compared with those of the solutions by Berger[6)]. The deflection by the discrete method is a little greater than Berger's solution.

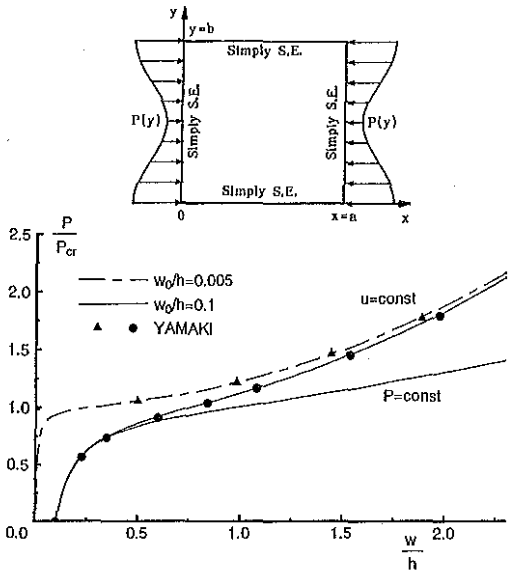

Fig.12 Load-deflection curves under edge compression (SSSS).

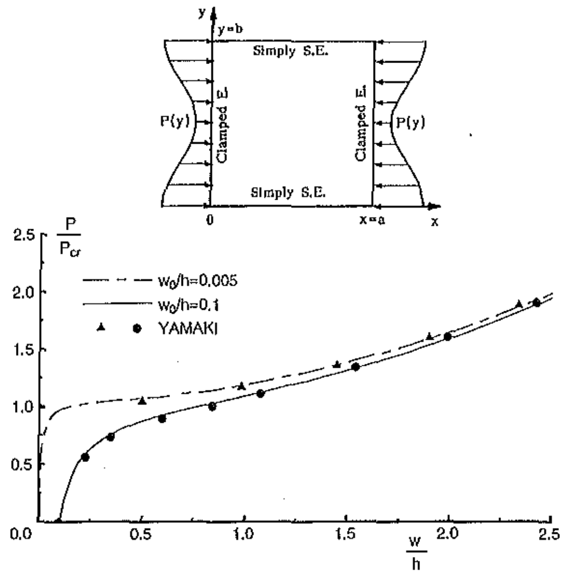

Fig.13 Load-deflection curves under edge compression (CSCS).

d) Plate under a concentrated load

Second, the present method is applied to the square plates under a concentrated load P at the center, with four clamped edges and with four simply supported edges. **Fig. 11** shows the load-deflection curves with respect to the maximum deflection when non-dimensional incremental load intensity is $\Delta Pa^2/Dh=50$.

(2) Rectangular plate subjected to edge compression

In the previous section, the rectangular plate subjected to lateral load has been treated. Here, the rectangular plate (h/a=0.01, ν=1/3) subjected to edge compression, with a small initial curvature (w_0/h=0.005,0.1) is considered.

a) Plate with four simply supported edges

First, the present method is applied to the simply supported square plates subjected to edge compression, with uniformly displaced edges and with uniformly loaded edges. **Fig.12** shows the load-deflection curves with respect to the maximum deflection at the center when the division $m=n=8$. In this figure the discrete solutions are compared with the double Fourier series solutions obtained by Yamaki[10]. It is found from this figure that a good agreement exists between these sets of results.

b) Plate with loaded edges clamped and the other edges simply supported

Next, the present method is applied to the square plate with loaded edges clamped and the other edges simply supported, and with uniformly displaced edges. **Fig.13** shows the load-deflection curves with respect to the maximum deflection at the center ($m=n=10$). The solutions obtained by Yamaki[10] are also plotted for comparison in **Fig.13**, and a good agreement is observed.

c) Plate with loaded edges simply supported and the other edges clamped

Fig.14 presents the computing results for a square plate with loaded edges simply supported and the other edges clamped, and with uniformly displaced edges. **Fig.14** shows the load-deflection curves with respect to the maximum deflection at point A ($m=n=8$). It is here assumed that the small initial deflection is two half-waves in the x-direction, because of a square plate buckling in two half-waves in the x-direction in this case. This figure also shows a comparison between the discrete solutions and a double Fourire series solutions obtained by Yamaki[10], and a good agreement exists between these sets of results.

7. CONCLUSIONS

The main conclusions can be summarized as follows.

(1) A general numerical method for the geometrical nonlinear problems of rectangular plates has been proposed, and the proposed method has been applied to the square plates

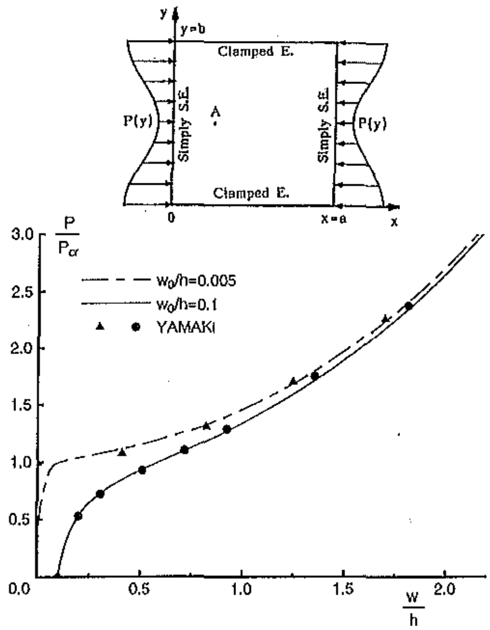

Fig.14 Load-deflection curves under edge compression (SCSC).

with three types of boundary conditions.

(2) The discrete solutions are obtained by transforming the differential equations into integral equations and applying numerical integrations, and they give the transverse shear forces, twisting moment, bending moments, rotations, deflection, in-plane displacements and membrane forces at all discrete points of the plate. Thus, the proposed method does not require prior assumption of the shape of the deflection of the plate.

(3) By utilizing the present method, the geometrical nonlinear problems for the rectangular plates having some of boundary and loading conditions can be treated with acceptable accuracy.

(4) In the proposed method, the size of the matrices of the simultaneous equation is reduced as well as the boundary element method. Furthermore, since the coefficients in Eqs.(6.A) and (6.B) can be independently calculated, CPU time can be reduced by using the parallel computer.

APPENDIX I

$$\Delta N_c=\Delta N_x\left(\frac{\partial^2 w}{\partial x^2}+\frac{\partial^2\Delta w}{\partial x^2}\right)+\Delta N_y\left(\frac{\partial^2 w}{\partial y^2}+\frac{\partial^2\Delta w}{\partial y^2}\right)+2\Delta N_{xy}\left(\frac{\partial^2 w}{\partial x\partial y}+\frac{\partial^2\Delta w}{\partial x\partial y}\right)$$

$$\Delta W_{xc}=\frac{1}{2}\left\{\left(\frac{\partial\Delta w}{\partial x}\right)^2+\nu\left(\frac{\partial\Delta w}{\partial y}\right)^2\right\}+\frac{\partial w}{\partial x}\frac{\partial\Delta w}{\partial x}+\nu\frac{\partial w}{\partial y}\frac{\partial\Delta w}{\partial y}$$

$$\Delta W_{yc}=\frac{1}{2}\left\{\left(\frac{\partial\Delta w}{\partial y}\right)^2+\nu\left(\frac{\partial\Delta w}{\partial x}\right)^2\right\}+\frac{\partial w}{\partial y}\frac{\partial\Delta w}{\partial y}+\nu\frac{\partial w}{\partial x}\frac{\partial\Delta w}{\partial x}$$

$$\Delta W_{xyc}=\frac{\partial\Delta w}{\partial x}\frac{\partial\Delta w}{\partial y}+\frac{\partial w}{\partial x}\frac{\partial\Delta w}{\partial y}+\frac{\partial w}{\partial y}\frac{\partial\Delta w}{\partial x}$$

APPENDIX II

$F_{111}=F_{123}=F_{134}=F_{156}=F_{167}=F_{188}=F_{278}=F_{377}=1$
$F_{212}=F_{225}=F_{233}=F_{247}=F_{266}=-F_{322}=-F_{331}=F_{386}=\mu$
$F_{146}=\nu$ $F_{257}=\nu\mu$ $F_{313}=\lambda_{xy}J$ $F_{314}=\mu(\lambda_y-\nu\lambda_x)\overline{D}$
$F_{315}=\mu(\lambda_x-\nu\lambda_y)\overline{D}$ $F_{345}=F_{354}=-I$ $F_{363}=-J$ $F_{372}=-K$
$F_{381}=-\mu K$ $f_{11}=\Delta\overline{q}+\Delta\overline{N}_c$
$F_{4911}=F_{41012}=F_{4129}=F_{41310}=1$ $F_{4119}=\nu$ $F_{51210}=\nu\mu$
$F_{5913}=F_{51011}=F_{51110}=F_{5139}=\mu$ $F_{61113}=-L_1$
$F_{61212}=-L_1$ $F_{61311}=-L_2$ $f_{211}=\mu\Delta W_{xc}$ $f_{212}=\mu\Delta W_{yc}$
$f_{213}=\mu\Delta W_{xyc}$ Other $F_{ijk}=f_{ij}=0$

APPENDIX III

$A_{p1}=\gamma_{p1}$ $A_{p2}=0$ $A_{p3}=\gamma_{p2}$ $A_{p4}=\gamma_{p3}$ $A_{p5}=0$
$A_{p6}=\nu\gamma_{p4}+\gamma_{p5}$ $A_{p7}=\gamma_{p6}$ $A_{p8}=\gamma_{p8}$ $A_{p9}=\nu\gamma_{p11}+\gamma_{p12}$
$A_{p10}=\gamma_{p13}$ $A_{p11}=\gamma_{p9}$ $A_{p12}=\gamma_{p10}$ $A_{p13}=0$
$B_{p1}=0$ $B_{p2}=\mu\gamma_{p1}$ $B_{p3}=\mu\gamma_{p3}$ $B_{p4}=0$ $B_{p5}=\mu\gamma_{p2}$
$B_{p6}=\mu\gamma_{p6}$ $B_{p7}=\mu(\gamma_{p4}+\nu\gamma_{p5})$ $B_{p8}=\gamma_{p7}$ $B_{p9}=\mu\gamma_{p13}$
$B_{p10}=\mu(\gamma_{p11}+\nu\gamma_{p12})$ $B_{p11}=\mu\gamma_{p10}$ $B_{p12}=0$ $B_{p13}=\mu\gamma_{p9}$
$C_{p1fg}=\mu(\gamma_{p3}+K_{fg}\gamma_{p8})$ $C_{p2fg}=\mu\gamma_{p2}+K_{fg}\gamma_{p7}$ $C_{p3fg}=J_{fg}$
$(\gamma_{p6}-\lambda_{xyfg}\gamma_{p1})$ $C_{p4fg}=I_{fg}\gamma_{p5}-\mu(\lambda_{yfg}-\nu\lambda_{xfg})\overline{D}_{fg}\gamma_{p1}$
$C_{p5fg}=I_{fg}\gamma_{p4}-\mu(\lambda_{xfg}-\nu\lambda_{yfg})\overline{D}_{fg}\gamma_{p1}$ $C_{p6fg}=-\mu\gamma_{p8}$
$C_{p7fg}=-\gamma_{p7}$ $C_{p8fg}=0$ $C_{p9fg}=0$ $C_{p10fg}=0$
$C_{p11fg}=L_{2fg}\gamma_{p13}$ $C_{p12fg}=L_{1fg}\gamma_{p12}$ $C_{p13fg}=L_{1fg}\gamma_{p11}$
$[\gamma_{pt}]=[\rho_{tp}]^{-1}$ ($p=1\sim8, t=1\sim8$ or $p=9\sim13, t=9\sim13$)
$\rho_{11}=\beta_{ii}$ $\rho_{12}=\mu\beta_{jj}$ $\rho_{13}=\beta_{ij}\lambda_{xyij}J_{ij}$
$\rho_{14}=\mu\beta_{ij}(\lambda_{yij}-\nu\lambda_{xij})\overline{D}_{ij}$ $\rho_{15}=\mu\beta_{ij}(\lambda_{xij}-\nu\lambda_{yij})\overline{D}_{ij}$
$\rho_{22}=-\mu\beta_{ij}$ $\rho_{23}=\beta_{ii}$ $\rho_{25}=\mu\beta_{jj}$ $\rho_{31}=-\mu\beta_{ij}$ $\rho_{33}=\mu\beta_{jj}$
$\rho_{34}=\beta_{ii}$ $\rho_{45}=-\beta_{ij}I_{ij}$ $\rho_{46}=\nu\beta_{ii}$ $\rho_{47}=\mu\beta_{jj}$
$\rho_{54}=-\beta_{ij}I_{ij}$ $\rho_{56}=\beta_{ii}$ $\rho_{57}=\nu\mu\beta_{jj}$ $\rho_{63}=-\beta_{ij}J_{ij}$
$\rho_{66}=\mu\beta_{jj}$ $\rho_{67}=\beta_{ii}$ $\rho_{72}=-\beta_{ij}K_{ij}$ $\rho_{77}=\beta_{ij}$ $\rho_{78}=\beta_{jj}$
$\rho_{81}=-\mu\beta_{ij}K_{ij}$ $\rho_{86}=\nu\beta_{ij}$ $\rho_{88}=\beta_{ii}$
$\rho_{911}=\beta_{ii}$ $\rho_{913}=\mu\beta_{jj}$ $\rho_{1011}=\mu\beta_{jj}$ $\rho_{1012}=\beta_{ii}$
$\rho_{119}=\nu\beta_{ii}$ $\rho_{1110}=\mu\beta_{jj}$ $\rho_{1113}=-\beta_{ij}L_{1ij}$ $\rho_{129}=\beta_{ii}$
$\rho_{1210}=\nu\mu\beta_{jj}$ $\rho_{1212}=-\beta_{ij}L_{1ij}$ $\rho_{139}=\mu\beta_{jj}$ $\rho_{1310}=\beta_{ii}$
$\rho_{1311}=-\beta_{ij}L_{2ij}$ $\beta_{ij}=\beta_{ii}\beta_{jj}$

$p=1\sim8$

$$a_{pijfd}=\sum_{t=1}^{8}\left\{\sum_{k=0}^{i}\beta_{ik}A_{pt}[a_{tk0fd}-a_{tkjfd}(1-\delta_{ki})]+\sum_{l=0}^{j}\beta_{jl}B_{pt}[a_{t0lfd}-a_{tilfd}(1-\delta_{lj})]+\sum_{k=0}^{i}\sum_{l=0}^{j}\beta_{ik}\beta_{jl}C_{ptkl}a_{tklfd}(1-\delta_{ki}\delta_{lj})\right\}$$

$$b_{pijgd}=\sum_{t=1}^{8}\left\{\sum_{k=0}^{i}\beta_{ik}A_{pt}[b_{tk0gd}-b_{tkjgd}(1-\delta_{ki})]+\sum_{l=0}^{j}\beta_{jl}B_{pt}[b_{t0lgd}-b_{tilgd}(1-\delta_{lj})]\right.$$

$$
\begin{aligned}
&\quad + \sum_{k=0}^{i}\sum_{l=0}^{j} \beta_{ik}\beta_{jl}C_{ptkl}b_{tklgd}(1-\delta_{ki}\delta_{lj})\Big\} \\
\Delta q_{pij} &= \sum_{t=1}^{8}\Big\{\sum_{k=0}^{i}\beta_{ik}A_{pt}[\Delta q_{tk0} - \Delta q_{tkj}(1-\delta_{ki})] \\
&\quad + \sum_{l=0}^{j}\beta_{jl}B_{pt}[\Delta q_{t0l} - \Delta q_{til}(1-\delta_{lj})] \\
&\quad + \sum_{k=0}^{i}\sum_{l=0}^{j}\beta_{ik}\beta_{jl}C_{ptkl}\Delta q_{tkl}(1-\delta_{ki}\delta_{lj})\Big\} \\
&\quad - \sum_{k=0}^{i}\sum_{l=0}^{j}\beta_{ik}\beta_{jl}A_{p1}(\Delta\bar{q}_{kl} + \Delta\bar{N}_{ckl})
\end{aligned}
$$

$p=9\sim13$

$$
\begin{aligned}
a_{pijfd} &= \sum_{t=9}^{13}\Big\{\sum_{k=0}^{i}\beta_{ik}A_{pt}[a_{tk0fd} - a_{tkjfd}(1-\delta_{ki})] \\
&\quad + \sum_{l=0}^{j}\beta_{jl}B_{pt}[a_{t0lfd} - a_{tilfd}(1-\delta_{lj})] \\
&\quad + \sum_{k=0}^{i}\sum_{l=0}^{j}\beta_{ik}\beta_{jl}C_{ptkl}a_{tklfd}(1-\delta_{ki}\delta_{lj})\Big\} \\
b_{pijgd} &= \sum_{t=9}^{13}\Big\{\sum_{k=0}^{i}\beta_{ik}A_{pt}[b_{tk0gd} - b_{tkjgd}(1-\delta_{ki})] \\
&\quad + \sum_{l=0}^{j}\beta_{jl}B_{pt}[b_{t0lgd} - b_{tilgd}(1-\delta_{lj})] \\
&\quad + \sum_{k=0}^{i}\sum_{l=0}^{j}\beta_{ik}\beta_{jl}C_{ptkl}b_{tklgd}(1-\delta_{ki}\delta_{lj})\Big\} \\
\Delta q_{pij} &= \sum_{t=9}^{13}\Big\{\sum_{k=0}^{i}\beta_{ik}A_{pt}[\Delta q_{tk0} - \Delta q_{tkj}(1-\delta_{ki})] \\
&\quad + \sum_{l=0}^{j}\beta_{jl}B_{pt}[\Delta q_{t0l} - \Delta q_{til}(1-\delta_{lj})] \\
&\quad + \sum_{k=0}^{i}\sum_{l=0}^{j}\beta_{ik}\beta_{jl}C_{ptkl}\Delta q_{tkl}(1-\delta_{ki}\delta_{lj})\Big\} \\
&\quad - \sum_{k=0}^{i}\sum_{l=0}^{j}\beta_{ik}\beta_{jl}\Delta\bar{W}_{cpkl} \\
\Delta\bar{W}_{cpkl} &= \gamma_{p11}\Delta W_{xckl} + \gamma_{p12}\Delta W_{yckl} + \gamma_{p13}\Delta W_{xyckl}
\end{aligned}
$$

REFERENCES

1) Th. von Kármán : Festigkeitsprobleme im Maschinenbau, Encyklopädie der Mathematischen Wissenschaften, Vol.4, p.394, 1910.
2) Marguerre,K. : Zur Theorie der gekrümmten Platte grosser Formänderung, Proc. 5th Intern. Congr. Appl. Mech., Cambridge, pp.93~101, 1938.
3) Kawai,T. and Yoshimura,N. : Analysis of large deflection of plates by finite element method, Int. Jour. for Numerical Methods in Engng. Vol.1, pp.123~133, 1969.
4) Schmidt,B. : Ein Geometrish und Physikalish Nichtlineares Finite-Element-Verfahren zur Berechnung von Ausgesteifen, Vorverformten Rechteckplatten, Der Stahlbau, Heft 1, S.13~21, 1979.
5) Way,S. : A laterally loaded clamped square plate with large deformation, Proc. 5th Int. Congr. Appl. Mech., Cambridge, pp.123~128, 1938.
6) Berger,H.M. : A new approach to the analysis of large deformation of plates, Journal of Applied Mechanics, Trans. ASME, Vol.22, pp.465~472, 1955.
7) Levy,S. : Bending of rectangular plates with large deflections, NACA, No.737, 1942.
8) Murray,D.W. and Wilson,E.L. : Finite element postbuckling analysis of thin elastic plates, AIAA Journal, Vol.7, No.10, pp.1915~1920, 1969.
9) Maeda,Y., Hayashi,M. and Mori,K. : Finite displacement analysis of thin plates by finite strip method, Proc. JSCE, No.316, pp.23~36, 1981 (in Japanese).
10) Yamaki,N. : Postbuckling behavior of rectangular plates with small initial curvature loaded in edge compression, Journal of Applied Mechanics, Trans. ASME. Vol.26, pp.407~414, 1959.
11) Coan,J.M. : Large deflection theory for plates with small initial curvature loaded in edge compression, Journal of Applied Mechanics, Trans. ASME, Vol.18, pp.143~151, 1951.
12) Sakiyama,T. and Matsuda,H. : Bending analysis of rectangular plate with variable thickness, Proc. JSCE, No.338, pp.21~28, 1983 (in Japanese).

(Received October 11, 1991)

矩形板の幾何学的非線形挙動解析

森田千尋・松田　浩・崎山　毅

本論文は、矩形板の幾何学的非線形問題のための一離散化数値解析法について述べたものである。有限変形を考慮した矩形板の変位ーひずみ関係により、矩形板の非線形挙動を支配する増分形の基礎微分方程式を導き、その基礎微分方程式に基づく、直接的で半解析的な、矩形板の非線形問題の一解析法を提示した。本法により、任意の荷重条件および境界条件の下での、矩形板の幾何学的非線形曲げ問題、後座屈問題を解析した。